



OPEN ACCESS

EDITED BY
Guoqiang Tang,
Wuhan University, China

REVIEWED BY
Veber Costa,
Federal University of Minas Gerais, Brazil
Ankit Ghanghas,
Swiss Re, Switzerland

*CORRESPONDENCE
Sheila Pournasiri Eero
✉ seero@Dewberry.com

RECEIVED 24 November 2025
REVISED 02 March 2026
ACCEPTED 16 March 2026
PUBLISHED 07 April 2026

CITATION
Eero SP, Sutley D and Dietrich AH (2026)
Event duration matters: spatial–
temporal patterns of United States daily
and multi-day precipitation extremes.
Front. Water 8:1753501.
doi: 10.3389/frwa.2026.1753501

COPYRIGHT
© 2026 Eero, Sutley and Dietrich. This is
an open-access article distributed under
the terms of the [Creative Commons
Attribution License \(CC BY\)](https://creativecommons.org/licenses/by/4.0/). The use,
distribution or reproduction in other
forums is permitted, provided the
original author(s) and the copyright
owner(s) are credited and that the
original publication in this journal is
cited, in accordance with accepted
academic practice. No use, distribution
or reproduction is permitted which does
not comply with these terms.

Event duration matters: spatial– temporal patterns of United States daily and multi-day precipitation extremes

Sheila Pournasiri Eero^{1*}, David Sutley¹ and
Alyssa Hendricks Dietrich²

¹Integrated Resilience Solutions, Dewberry, Denver, CO, United States, ²Integrated Resilience
Solutions, Dewberry, Fairfax, VA, United States

Understanding the dynamics of extreme precipitation is essential for assessing flood risk, designing resilient infrastructure, and adapting to climate variability. This study examines the spatial and temporal characteristics of single-day and multi-day precipitation extremes across the contiguous United States using station-based observations from 1979 to 2023. The analysis is based on three categories: (i) daily (single 1-day) maxima, (ii) 3-day and 5-day accumulations, and (iii) event-based wet-spell accumulation. Using these indicators, we assess variability, event structure, and seasonality across the nine National Centers for Environmental Information (NCEI) climate regions. We first compare how precipitation indicators vary across durations and regions, including the contribution of the wettest day to multi-day events and the temporal co-occurrence of maximum 1-day and multi-day peaks. We then examine seasonal timing and trend patterns. Finally, we explore how duration-dependent extremes align with documented regional storm regimes. The results reveal distinct spatial and temporal contrasts between indicators, as well as among climate regions, characterizing how each indicator captures different, though partly overlapping, aspects of United States (U.S.) precipitation extremes. These spatial and seasonal differences are broadly consistent with regional storm regimes and precipitation characteristics documented in prior studies. By jointly analyzing 1-day and multi-day extremes using a unified set of indicators, this study provides a regionally nuanced perspective on the multidimensional nature of extreme precipitation and highlights the importance of precipitation persistence alongside peak intensity for flood-risk characterization and adaptation planning.

KEYWORDS

extreme precipitation, flood risk, GHCN-D observations, multi-day precipitation, NCEI climate regions, seasonality, spatial variability, wet spells

1 Introduction

Extreme precipitation events significantly heighten hydrological risks by increasing flooding, overwhelming water infrastructure, and creating complex water management issues (Coelho et al., 2022; Nguyen et al., 2025; U.S. Environmental Protection Agency, 2025). These episodes also intensify landslides and cascading infrastructure failures (Dharmarathne et al., 2024) and disrupt ecosystems and human livelihoods (Dharmarathne et al., 2024; Dhawale et al., 2024; El Kenawy, 2024). Extreme rainfall can occur as short-lived, single-day events or as

prolonged multi-day accumulations, each with distinct types of hydrologic hazards that manifest in different ways. While single-day extremes often dominate rainfall records and design standards (Nguyen et al., 2025), multi-day precipitation events such as 3-day, 5-day, or even extended wet accumulations can be equally or more damaging due to their cumulative effects. Prolonged multi-day rainfall can lead to compound floods, dam and levee failures, and landslides, overwhelming both natural and engineered water-management systems (Moore et al., 2021; Wan et al., 2021; Ye et al., 2021; Yu et al., 2023; Fereshtehpour et al., 2025; National Oceanic and Atmospheric Administration, National Weather Service, 2025; Wang, 2025). Although intense, short-duration storms may trigger flash flooding, multi-day events often produce cascading effects by saturating soils, increasing overall runoff, and amplifying the likelihood of widespread flooding and landslides (Zhang and Villarini, 2020; Du et al., 2022; Jin et al., 2024; U.S. Environmental Protection Agency, 2025).

Many major U.S. flooding events are directly linked to prolonged periods of rainfall. For instance, during the historic Midwest floods of 2017 and 2019, persistent rainfall over several weeks caused severe infrastructure damage and agricultural losses (Heimann et al., 2018; National Oceanic and Atmospheric Administration, 2019; Kraft et al., 2023; Nguyen et al., 2025). Similarly, in May–June 2019, prolonged heavy rainfall across the South-Central U.S. produced record flooding along the Arkansas River and its tributaries, as sustained moisture transport and recurrent storm systems generated consecutive high-yield rainfall events, which overwhelmed catchments and flood-control structures (Lewis and Trevisan, 2019; Williams and Lewis, 2020; NOAA Weather Forecast Office, 2025). Multi-day rainfall also played a central role in the devastating 2013 Colorado floods, where persistent upslope flow of moist air produced hybrid stratiform–convective storms (Association of State Dam Safety Officials, 2013; Uccellini, 2014; Gochis et al., 2015; Tye and Cooley, 2015; Friedrich et al., 2016; Dougherty and Rasmussen, 2019). Comparable dynamics occurred in the Pagosa Springs flood in Colorado during the October 10–14, 2025, when a moisture-laden storm system produced several consecutive days of rainfall, leading to cumulative runoff, raised river levels, and overtopping of the San Juan River and its tributaries with resulting infrastructure damage (Western Water Assessment, 2025). These events underscore that it is not only isolated single-day maxima, but also the accumulation of rainfall over multiple days, which causes the most damaging flood outcomes.

The risk of such multi-day extremes is often amplified by interacting hazards, including preconditioning (e.g., saturated soils prior to a storm), multivariate interactions (e.g., precipitation and coastal flooding), temporal clustering of storms, and spatially congruent extremes (Zscheischler et al., 2018; Bevacqua et al., 2021; Ganguli et al., 2022; Hao, 2022; Zscheischler et al., 2022; Fereshtehpour et al., 2025). Previous studies have reported increases in the frequency and intensity of multi-day precipitation extremes in parts of the U.S., including the Midwest and Northeast (Changnon et al., 2001; Roque-Malo and Kumar, 2017; Du et al., 2022; Nguyen et al., 2025). Relying solely on single-day rainfall thresholds to inform flood risk assessment, while overlooking prolonged wet periods and antecedent soil moisture, is increasingly viewed as outdated (Ye et al., 2021; Yu et al., 2023; Hwang and Lall, 2024). Growing evidence shows that antecedent wetness and event persistence, rather than isolated daily extremes, are stronger predictors of flood severity (Luong et al., 2021; Ye et al., 2021; Jiang et al., 2022).

Beyond flood generation, incorporating precipitation across multiple durations is essential for improving hydrologic and

hydraulic modeling frameworks. Reliance on single-day events overlooks the cumulative watershed response to prolonged wet periods and underestimates flood potential. Analyzing precipitation across multiple durations can enable the identification of regions with similar hydrologic responses under persistent rainfall and may facilitate transferring the insights across watersheds with comparable flood-generation mechanisms. Such cross-regional synthesis could form the basis of a systematic national framework for evaluating flood hazards, while clarifying the meteorological and hydrologic processes that create these patterns (Stein et al., 2020; Brunner et al., 2021; Ma et al., 2021; Moges et al., 2022; Trambly et al., 2022; Yeh and Chen, 2022; Shen and Chui, 2023; Tarasova et al., 2023).

The challenges articulated by Clark et al. (2016) are central to advancing hydrologic modeling beyond individual catchments toward a more generalizable, transferable approach. They emphasize developing a coherent, theory-based understanding of macroscale hydrology by identifying consistent watershed behaviors, formulating general process laws, and unifying explanations within a common process-based perspective. Within this broader context, incorporating cumulative and multi-duration precipitation statistics provides diagnostic insight into rainfall persistence and accumulation patterns. Such characteristics are relevant for distinguishing precipitation regimes that may contribute differently to flood-generation processes (e.g., short-duration intensity-driven events versus persistence-driven saturation events).

Unlike traditional approaches that often emphasize peak daily intensity (appropriate for flash-flood analysis but less suited to delayed hydrologic responses) multi-day precipitation indicators (e.g., 3-day, 5-day) and event-based wet-spell accumulation provide diagnostic insight into duration-dependent precipitation structure, and flood-generation processes across regions. Embedding such statistics within operational frameworks—including floodplain mapping, reservoir and dam management, stormwater design, and long-duration flood forecasting—can help translate process-based hydrologic understanding into actionable planning tools, enabling insights from one region to inform adaptive strategies elsewhere in the U.S. (Stein et al., 2020; Trambly et al., 2022; Banerjee et al., 2023; Brandi et al., 2023; Eilander et al., 2023; Tarasova et al., 2023). Yet, despite growing evidence of increasing extreme precipitation intensity and frequency in the U.S. (Banerjee et al., 2023; Brandi et al., 2023; Dettinger and Horton, 2023), relatively few studies have systematically examined these dynamics across multiple durations and regions. Most existing studies isolate single-day precipitation extremes, leaving a critical gap in characterizing and comparing the spatial and temporal variability of single-day and multi-day extremes across regions.

To better understand the spatial and temporal patterns of extreme precipitation, we analyzed station-based daily gauge observations to derive maximum 1-day, 3-day, and 5-day extremes, as well as accumulation during the longest wet spell, across the nine NCEI climate regions of the contiguous U.S. Considering both annual and seasonal perspectives, we evaluate:

- The variability of precipitation extremes across durations and regions,
- The percentage contribution of the wettest day to the corresponding multi-day total,
- The temporal co-occurrence of single-day maxima and multi-day events, and
- Seasonal timing and exploratory analysis of trend patterns across durations and regions.

While previous studies have examined extreme precipitation at individual durations, specific regions, or through formal scaling and frequency-analysis methods, this study evaluates magnitude, intra-event concentration (wettest-day contribution), co-occurrence behavior, seasonal timing, and persistence-based wet-spell accumulation within a consistent, gauge-based national comparison. By analyzing fixed-window extremes (1-, 3-, and 5-day) alongside accumulation during the longest wet spell, this study provides a regional comparison of the structural behavior of U.S. precipitation extremes and identifies contrasts between intensity-dominated and persistence-dominated precipitation patterns that are not apparent when durations are considered in isolation.

2 Data and methods

2.1 Data

We used daily precipitation data from the Global Historical Climatology Network-Daily (GHCN-D) to define precipitation indicators across the nine NCEI climatological regions. The GHCN-D database, developed by NCEI, is the most comprehensive collection of daily precipitation records for the U.S. (Menne et al., 2012). GHCN-D observations have a sensitivity of 0.1 mm and undergo rigorous quality control procedures to ensure data integrity (Durre et al., 2010). For the analysis, we selected stations with at least 90% data completeness over the period 1979–2023 (Figure 1).

2.2 Defining precipitation indicators

To characterize precipitation patterns and variability, we developed a suite of indicators capturing key aspects of precipitation behavior, including magnitude, percentage contribution, co-occurrence, and timing, as summarized in Table 1.

The magnitude indicators including maximum 1-day precipitation (MAX1D), maximum 3-day precipitation total (MAX3D), maximum 5-day precipitation total (MAX5D), and maximum precipitation accumulated during the longest continuous (MAXWD) were calculated annually and for each of the four traditional seasons: Winter (December, January, February: DJF), Spring (March, April, May: MAM), Summer (June, July, August: JJA), and Fall (September, October, November: SON) over the 1979–2023 period. These values are expressed in millimeters (mm) of precipitation. MAX1D, MAX3D, and MAX5D represent indicators computed over fixed-length accumulation windows, whereas MAXWD represents the maximum accumulation over an event-based wet spell with variable (random) duration. MAXWD is therefore not treated as additional fixed time scales, but rather as stochastic event-based accumulation indicators that characterize precipitation persistence and clustering. Comparisons between fixed-window extremes and wet-spell accumulation are intended as diagnostic contrasts in event structure, not as formal scaling relationships or probabilistic equivalence across duration constructs.

Thus, wet spells are not treated as an additional fixed time scale, but rather as stochastic indicators of precipitation persistence and clustering that complement fixed-window extremes.

The MAXWD represents the total precipitation accumulated during the longest continuous wet spell in a given year or season. If multiple wet

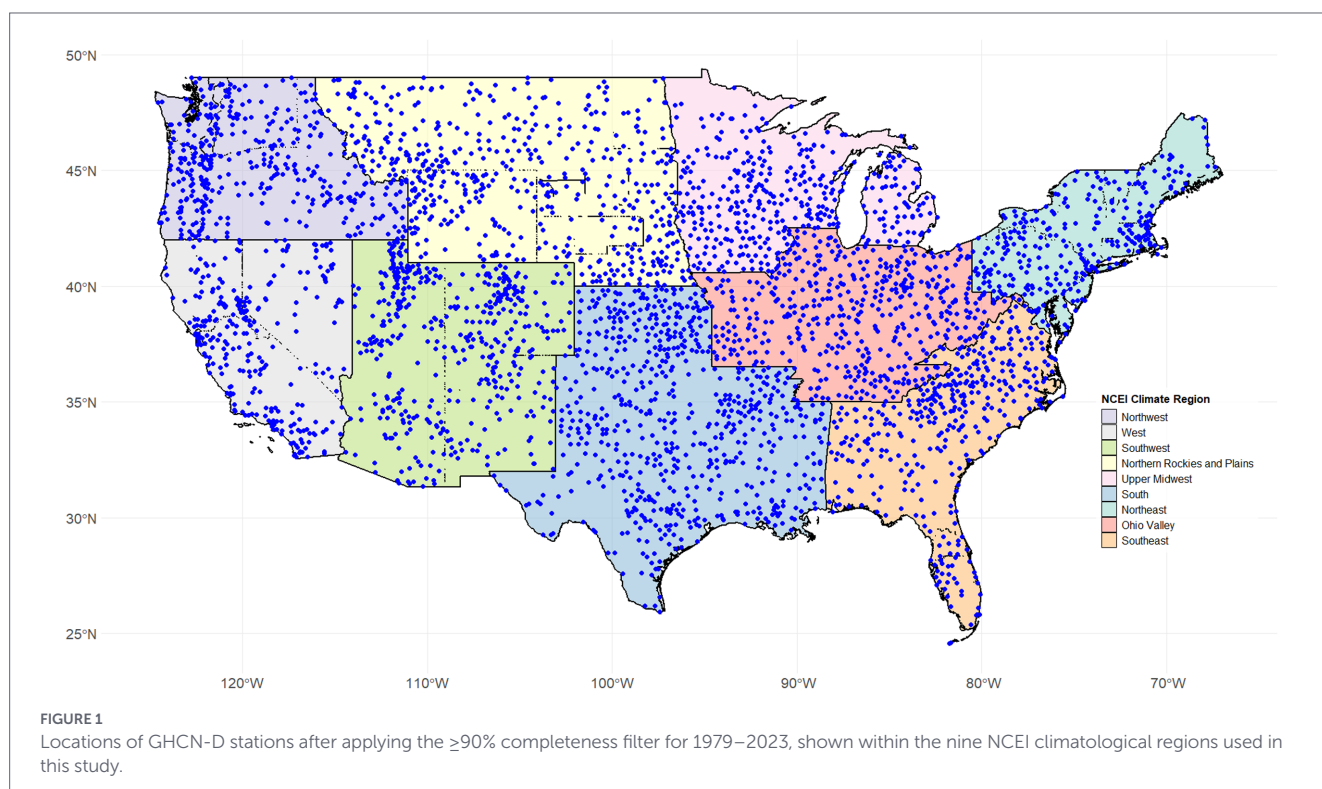


TABLE 1 Precipitation indicators used in this study, categorized by magnitude, wettest-day contribution, co-occurrence, and timing.

Category	Indicator	Abbreviation	Unit
Magnitude (annual and seasonal)	Maximum 1-day precipitation	MAX1D	Millimeter (mm)
	Maximum 3-day precipitation	MAX3D	
	Maximum 5-day precipitation	MAX5D	
	Maximum accumulated precipitation during the longest wet spell	MAXWD	
Percentage contribution (annual)	Contribution of the wettest day to MAX3D	CWM3D	Percent
	Contribution of the wettest day to MAX5D	CWM5D	
	Contribution of the wettest day to MAXWD	CWMWD	
Co-occurrence	Co-occurrence of the absolute maximum 1-day rainfall with the wettest day in MAX3D	CM1M3D	1 and 0
	Co-occurrence of the absolute maximum 1-day rainfall with the wettest day in MAX5D	CM1M5D	
	Co-occurrence of the absolute maximum 1-day rainfall with the wettest day in MAXWD	CM1MWD	
Timing	Date of the annual MAX1D	DMAX1D	Month/Day/Year
	Date of the wettest day in MAX3D	DMAX3D	
	Date of the wettest day in MAX5D	DMAX5D	
	Date of the wettest day in MAXWD	DMAXWD	

Fixed-window extremes (MAX1D, MAX3D, MAX5D) are computed over 1-, 3-, and 5-day accumulation windows, respectively. MAXWD denotes maximum precipitation accumulated during the longest wet spell within a year or season.

spells share the same maximum duration within a year or season, the spell with the largest total precipitation is selected. We defined a wet day as any day with precipitation greater than 0 mm (precipitation > 0) rather than using a strict threshold of 1 mm. We made this decision to ensure that extreme multi-day precipitation events are fully captured, even if one or more days within the event receive slightly less than 1 mm of rainfall. Using precipitation ≥ 1 mm could artificially break up extreme wet periods, potentially excluding significant events due to small daily precipitation amounts. Given that extreme precipitation analysis often relies on identifying the longest and most intense wet periods, this approach provides a more robust representation of continuous heavy rainfall events, ensuring that their full impact is considered.

To quantify the contribution of a single intense day to each multi-day extreme, we calculated the percentage contribution of the wettest day to the corresponding multi-day total. Specifically, CWM3D, CWM5D, and CWMWD represent the ratio (in %) of the wettest single day's precipitation within each maximum 3-day, 5-day, and wet-period event to the total precipitation of that event.

- CWM3D: (precipitation of wettest day within MAX3D/MAX3D total) $\times 100$
- CWM5D: (precipitation of wettest day within MAX5D/MAX5D total) $\times 100$
- CWMWD: (precipitation of wettest day within MAXWD/MAXWD total) $\times 100$

These contribution indicators quantify how much of a multi-day extreme is driven by a single wettest day. A higher percentage indicates that the event is strongly dominated by 1 day of intense rainfall, whereas lower percentages indicate that precipitation was more evenly distributed across the event duration.

We also examined the temporal co-occurrence between 1-day and multi-day extremes by identifying how often the annual MAX1D coincided with the wettest day within MAX3D, MAX5D, and MAXWD. These co-occurrence indicators (CM1M3D, CM1M5D, and CM1MWD) indicate whether daily peaks contribute to broader multi-day extremes or persistence-based extremes.

Finally, we identified the calendar dates corresponding to each extreme precipitation event: DMAX1D (maximum 1-day precipitation), DMAX3D (the wettest day within the maximum 3-day total), and DMAX5D (the wettest day within the maximum 5-day total). These dates were used to examine the seasonal and temporal distribution of precipitation extremes.

2.3 Statistical analysis of spatial precipitation variability

To explore how precipitation indicators vary spatially across climate regions, we analyzed the coefficient of variation (CV) for each magnitude indicator listed in Table 1. The CV is particularly suited for this purpose as it normalizes the standard deviation (SD) by the mean, enabling meaningful comparisons across variables with differing scales (Neal and Phillips, 2011; Addisu et al., 2015; Pournasiri et al., 2018). While the SD quantifies the spread around the mean, the CV expresses this spread as a proportion of the mean, making it ideal for evaluating variability in magnitude indicators (MAX1D, MAX3D, MAX5D, and MAXWD). For each station, we first calculated the SD and mean, followed by CV as the ratio of standard deviation to the mean, multiplied by 100. This provided a standardized measure of variability across stations and climate regions.

As the pooled CV data for all stations within each climate region were skewed, we applied a log transformation to the CV values to improve distributional symmetry, which reduces skewness and limits the influence of extreme values when comparing variability across the nine NCEI climate regions (Pournasiri et al., 2018). At the same time, raw-scale CV values are retained and evaluated to preserve physically interpretable variability and information related to skewness and tail behavior (Supplementary Table S2), which are relevant in the context of extreme precipitation variability (Koutsoyiannis, 2025).

Normality of log-transformed CV values was evaluated using the Shapiro–Wilk test (Shapiro and Wilk, 1965; Agbonaye and Izinyon, 2021). As most distributions did not meet the assumption of normality (Supplementary Table S1), we proceeded with the non-parametric paired Wilcoxon signed-rank test (Wilcoxon, 1945; Uchale and Singh, 2025) to compare the log-transformed CVs of MAX1D, MAX3D,

MAX5D, and MAXWD within each climate region. These tests assessed whether differences in variability across event durations were statistically significant, using a significance level of $\alpha = 0.05$. As maxima derived from overlapping accumulation windows are not fully independent, and given the relatively large number of stations within each region, statistical significance is interpreted as evidence of distributional differences rather than distinct physical regimes. Accordingly, interpretation emphasizes effect sizes and distributional contrasts rather than p -values alone, as large samples can produce very small p -values even when practical differences are modest (Serinaldi et al., 2018).

To complement hypothesis testing, we assessed effect size using the rank-biserial correlation, which quantifies the practical significance of observed differences. Effect sizes were computed from log-transformed CV values to ensure consistency with test inputs, while their signs were derived from raw CV differences to retain the direction of variability. A positive effect size indicates that the first indicator in a pair exhibits greater variability than the second, whereas a negative value suggests the opposite.

This combined approach highlights both the statistical and hydrological relevance of regional differences in precipitation variability.

As variability was assessed at the station level and subsequently summarized within each NCEI climate region, regional statistics are based on pooling station-level indicator values and therefore implicitly assign equal weight to each station. While using a common analysis period (1979–2023) and a $\geq 90\%$ data completeness threshold reduces temporal and missing-data biases, differences in station density and hydroclimatic heterogeneity across regions may influence the representativeness of pooled distributions. Importantly, primary results are presented as station-level distributions (e.g., boxplots and density plots) rather than single regional means; thus, the analysis is intended to characterize within-region variability in station behavior rather than area-weighted regional climate statistics. Alternative spatial aggregation strategies, such as area-weighted or gridded approaches, represent a valuable extension for assessing sensitivity to spatial sampling and are beyond the scope of this study.

2.4 Temporal trends

To detect temporal trends in precipitation magnitude indicators, we used the Mann-Kendall (MK) trend test, a non-parametric method

widely used in hydrology and climatology (Mann, 1945; Kendall, 1975; Pournasiri and Pal, 2016). It does not assume a normal distribution and is robust against outliers, making it suitable for detecting gradual changes in precipitation magnitude over time. The MK test provides Kendall's tau (τ) as a measure of trend strength and direction, with statistical significance assessed using a p -value threshold of 0.05.

3 Results

3.1 Variability and event structure

This section presents a detailed evaluation of how extreme precipitation variability differs across climate regions and event durations, using a combination of statistical analysis and visual assessments. The findings provide a regionalized perspective on the spatial and temporal dynamics of rainfall extremes.

3.1.1 Regional variability across different durations

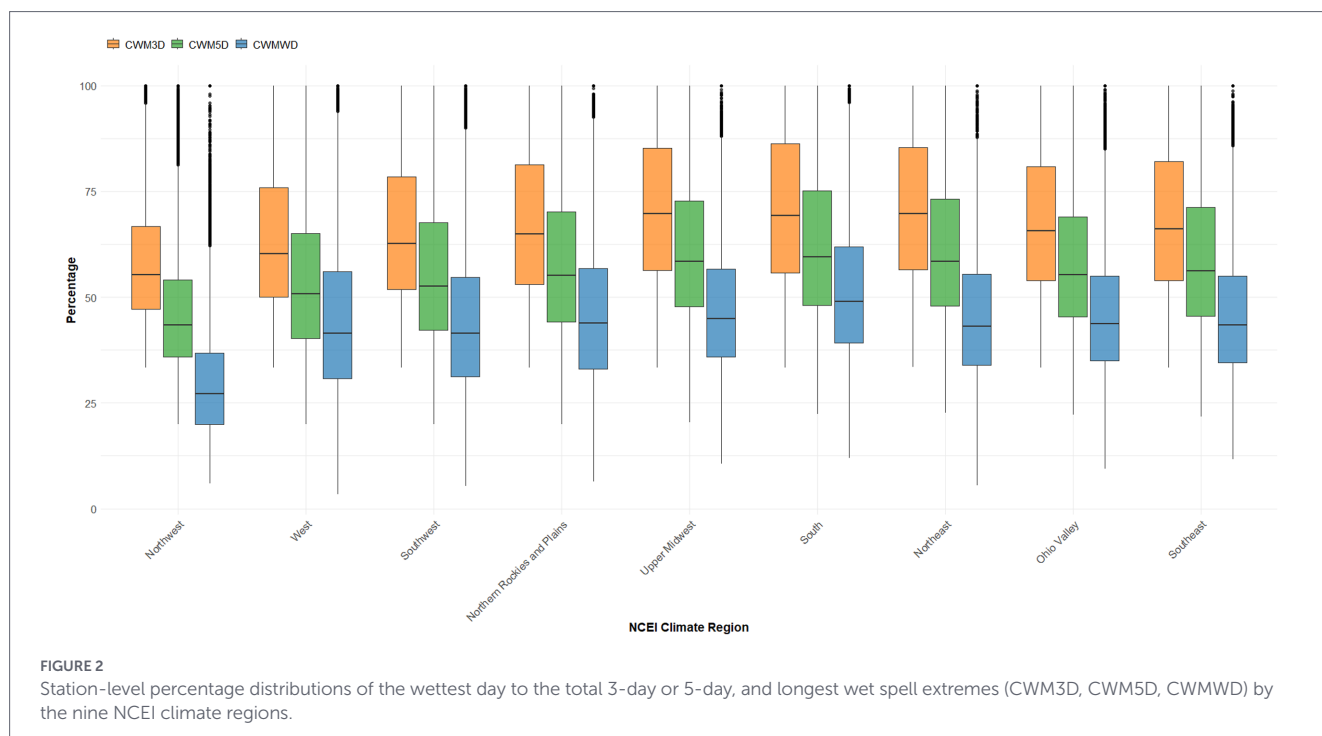
Table 2 presents the results of paired Wilcoxon signed-rank tests and effect size comparisons for log-transformed CV values of precipitation magnitude indicators across the nine NCEI climate regions. Effect sizes reveal regionally varying contrasts in variability across precipitation indicators across the U.S., with p -values reported for reference and interpreted along with the effect sizes.

In general, MAX1D exhibits higher variability than MAX3D and MAX5D. This is reflected in the predominantly positive effect sizes in comparisons between MAX1D and MAX3D, as well as between MAX3D and MAX5D. However, the magnitude and direction of these contrasts vary across regions. For instance, in the South, the difference between MAX1D and MAX3D is negligible and not significant (effect size = -0.003), while in the West and Southwest, effect sizes are small or negative, indicating comparable or greater variability at longer durations. These results demonstrate that changes in variability with increasing duration are region dependent, both in magnitude and direction. The strongest contrasts in variability across accumulation durations are observed in the Northeast, Southeast, and Upper Midwest, where effect sizes for MAX1D vs. MAX5D exceed 0.50. In

TABLE 2 Pairwise comparisons of log-transformed CV for MAX1D, MAX3D, MAX5D, and MAXWD across the nine NCEI climate regions using the paired Wilcoxon signed-rank test.

Region	MAX1D vs. MAX3D	MAX1D vs. MAX5D	MAX3D vs. MAX5D	MAX1D vs. MAXWD	MAX3D vs. MAXWD	MAX5D vs. MAXWD
Northwest	0.44 (3.62E-17)	0.48 (2.36E-20)	0.35 (2.05E-11)	-0.77 (2.86E-49)	-0.82 (5.68E-55)	-0.83 (6.14E-57)
West	-0.14 (2.26E-02)	-0.25(4.43E-05)	-0.33 (6.83E-08)	-0.84 (2.68E-43)	-0.86 (3.77E-45)	-0.87 (2.18E-45)
Southwest	0.07 (1.18E-01)	-0.04 (4.61E-01)	-0.02 (6.72E-01)	-0.81 (3.63E-65)	-0.83 (2.98E-67)	-0.82 (4.73E-67)
Northern Rockies and Plains	0.31 (4.03E-12)	0.41 (4.44E-20)	0.33 (1.38E-13)	-0.82 (9.62E-78)	-0.84 (4.11E-80)	-0.85 (1.45E-81)
Upper Midwest	0.39 (8.40E-14)	0.52 (5.02E-23)	0.47 (5.39E-19)	-0.82 (1.96E-54)	-0.82 (8.66E-55)	-0.82 (5.80E-55)
South	-0.003 (9.62E-01)	0.12 (2.89E-03)	0.30 (1.92E-14)	-0.84 (1.22E-98)	-0.85 (1.20E-100)	-0.85 (9.63E-103)
Northeast	0.35 (3.96E-09)	0.57 (7.98E-22)	0.63 (9.69E-26)	-0.85 (3.98E-46)	-0.86 (1.01E-46)	-0.86 (3.77E-47)
Ohio Valley	0.21 (4.42E-06)	0.33 (1.96E-12)	0.32 (5.14E-12)	-0.85 (3.98E-74)	-0.86 (4.84E-76)	-0.86 (1.46E-76)
Southeast	0.26 (3.48E-07)	0.52 (1.79E-23)	0.65 (1.31E-35)	-0.83 (7.18E-57)	-0.84 (1.68E-58)	-0.85 (2.46E-60)

Each cell reports the rank-biserial correlation effect size on the first line and the corresponding p -value on the second line in parentheses. Cell color indicates direction only: blue = positive effect size (first-listed duration has higher CV) and pink = negative effect size (second-listed duration has higher CV). Statistical significance is assessed at $\alpha = 0.05$ (i.e., $p < 0.05$).



contrast, regions such as the South, Southwest, and West show minimal differences (effect sizes close to zero or negative), suggesting more uniform variability across durations.

While comparisons among MAX1D, MAX3D, and MAX5D typically yield small to moderate effect sizes (ranging from -0.003 to 0.65), suggesting gradual changes in variability across increasing duration, a more pronounced contrast is observed when these indicators are compared with MAXWD. Comparisons involving MAXWD consistently show large and strongly negative effect sizes (often < -0.80) across all regions, indicating much greater variability in precipitation accumulated during the longest wet spell (MAXWD) relative to block-duration extremes. This elevated variability is consistent with the stochastic and variable-duration nature of wet spells.

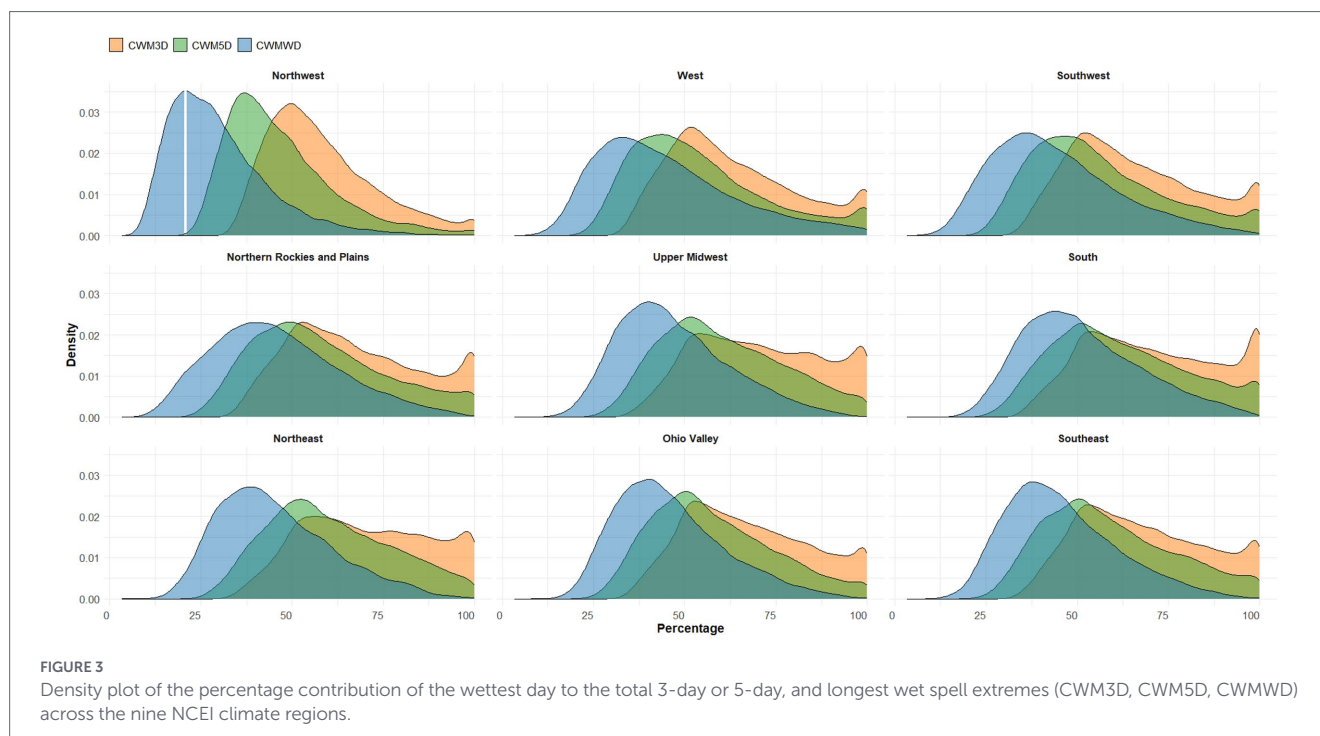
Descriptive statistics (Supplementary Table S2) reinforce and expand the findings, providing a broader view of regional variability. Across most climate regions, mean CV decreases from MAX1D to MAX3D to MAX5D, indicating reduced variability with longer accumulation durations. However, some regions, particularly the West, deviate from this pattern, with variability increasing at longer durations, likely reflecting the unique regional precipitation dynamics. In contrast, MAXWD consistently exhibits higher mean CV values than all other indicators (ranging from 52.15 in the Northwest to 67.44 in the West), heightening the greater interannual variability associated with persistence-based precipitation accumulation. SD of CV values further reveals spatial consistency versus heterogeneity within regions. Regions such as the Northwest, Southwest, and Upper Midwest have larger SD values, indicating greater spatial variability in precipitation behavior across stations. Conversely, the Northeast and Ohio Valley exhibit smaller SD values, suggesting more spatially uniform variability. Although MAXWD often has slightly lower SD values than MAX1D, it follows a similar regional pattern. This suggests that variability differs not only in magnitude across indicators and regions but also in the consistency with which it is expressed across stations.

3.1.2 Wettest day contribution to multi-day events

We analyzed the contribution of the wettest day to total precipitation over 3-day, 5-day, and longest wet-spell using the indicators CWM3D, CWM5D, and CWMWD, respectively. This analysis reveals how much single-day rainfall dominates within multi-day precipitation extremes and how that dominance varies across different climate regions.

Figure 2 presents the percentage contribution of the wettest day for each of the three durations across the nine NCEI climate regions. The x-axis represents the climate regions, while the y-axis indicates the contribution of the wettest day. Each region includes three boxplots: orange for CWM3D, green for CWM5D, and blue for CWMWD. Across most regions, the median contribution of the wettest day is highest for CWM3D and declines with increasing accumulation duration, highlighting that single-day extremes tend to dominate more strongly over shorter durations. Regions such as the Upper Midwest, South, and Northeast exhibit the highest median contributions for both CWM3D ($\sim 70\%$) and CWM5D ($\sim 60\%$), accompanied by wider interquartile ranges, evidence of strong but spatially variable single-day rainfall control. Across all regions, CWMWD values are consistently lower than those for CWM3D and CWM5D, with medians ranging from about 27% in the Northwest to roughly 49% in the South. As expected from the indicators' definition, the wettest-day share generally decreases with increasing accumulation length. However, extreme outliers—where 1 day accounts for nearly 100% of multi-day precipitation—occur in several regions (notably the South, Northern Rockies and Plains, and Northwest).

We note that the decreasing ordering in Figure 2 (CWM3D > CWM5D > CWMWD) is partly an expected consequence of the metric definition: as the accumulation window increases, precipitation is distributed across more days, and the maximum single-day share typically declines even if event structure remains unchanged. Accordingly, the physically informative signal lies not in the ordering itself, but in the regional contrasts in precipitation



concentration—including differences in medians, interquartile ranges, distributional shape, and the prevalence of extreme dominance events approaching 100%. For reference, under a purely even distribution of rainfall across days, the wettest-day share would equal $1/n$ of the total ($\approx 33\%$ for 3-day totals and 20% for 5-day totals). Departures above these reference values indicate stronger single-day dominance, whereas values closer to them reflect greater multi-day persistence.

Supplementary Table S3 summarizes descriptive statistics of CWM3D, CWM5D, and CWMWWD (%) across all climate regions. Consistent with Figure 2, the mean and median values decrease with longer duration, while SDs remain large, reflecting spatial heterogeneity in precipitation structure. The Count 100 column quantifies stations where a single day accounted for all precipitation (100%) within a 3-day, 5-day, or maximum wet-day event, highlighting rare but hydrologically pronounced single-day dominance.

At the same time, Figure 2 and Supplementary Table S3 shows that 40–70% of total precipitation in most 3-day or 5-day events comes from days other than the wettest one, while CWMWWD indicates a broader contribution (50–75%).

Figure 3 complements these findings by illustrating regional differences in precipitation structure. It shows density distributions of the percentage contribution of the wettest single day to total precipitation during the 3-day, 5-day, and maximum wet-day durations (CWM3D, CWM5D, CWMWWD) across the nine NCEI climate regions. In each density plot, the x-axis represents the wettest day's percentage contribution, and the y-axis shows its distribution across stations. These distributions reveal how strongly a single day influences short-duration precipitation totals, highlighting notable regional contrasts in the dominance of extreme daily events. Across all regions, CWM3D distributions (orange) are right-skewed with higher percentages clustering above 50%, reinforcing the strong influence of single-day rainfall on short accumulation duration. Conversely, the CWM5D and CWMWWD curves (green and blue) shift to the left, indicating that as duration increases, precipitation becomes more evenly distributed among

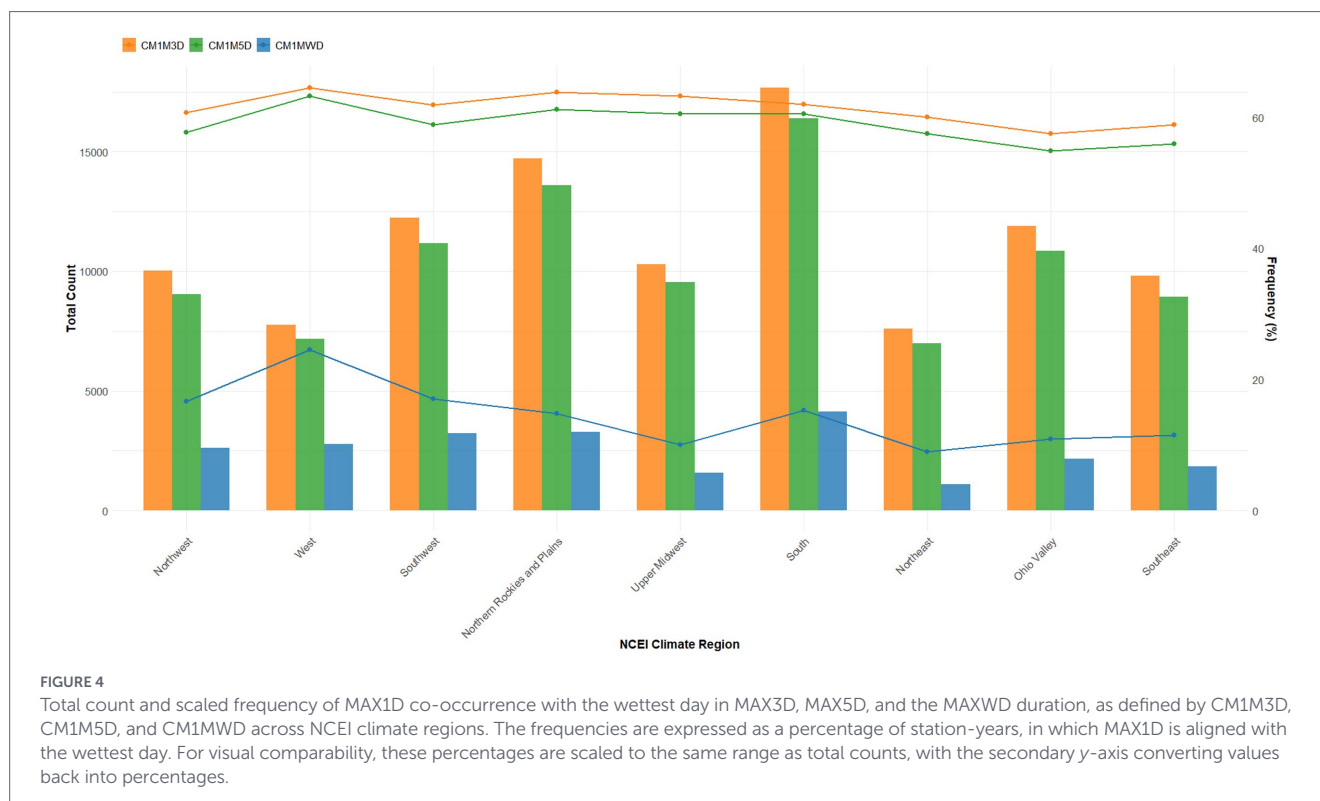
multiple days. This shift is particularly evident in the Northwest, where both CWM5D and CWMWWD densities form narrow, sharp peaks around 25–45%, signifying highly consistent multi-day rainfall structures. In contrast, the South, Upper Midwest, and Northeast display broader, flatter distributions, reflecting greater variability among stations and more localized dominance events. The West also shows a flatter shape than the Northwest, suggesting intermediate behavior, less uniform than the Northwest but less variable than the humid eastern regions.

Secondary peaks—most noticeable in the CWM3D distributions—appear in several regions (e.g., South, Northern Rockies and Plains, West, and Southwest) and align with the Count100 results in Supplementary Table S3. These peaks represent rare events where nearly all precipitation during a multi-day duration occurred within a single day.

The results show that the wettest day plays a greater role in 3-day events, with its contribution decreasing as the event duration increases. Regional variability—particularly the strong dominance in the South and Upper Midwest versus the consistent, low-variance patterns in the Northwest—underscores that precipitation structure and variability are region-specific. The considerable and regionally variable contribution from non-peak days underscores the need to account for cumulative precipitation when assessing flood risk and other hydrologic processes.

3.1.3 Co-occurrence of max 1-day and multi-day extremes

This section examines the co-occurrence between the maximum 1-day precipitation event (MAX1D) and the wettest day within the 3-day, 5-day, and maximum wet day durations, using the indicators CM1M3D, CM1M5D, and CM1MWD (as defined in Sections 2.2). Figure 4 presents both the total count and scaled frequency of co-occurrence across nine climate regions, while Supplementary Table S4 provides supporting summary statistics.



Across all regions, co-occurrence is highest for the 3-day duration (orange), where the MAX1D most frequently aligns with the wettest day (mean frequencies ranging from 57 to 65%). For example, the West (65%), Northern Rockies and Plains (64%), and Upper Midwest (63%) exhibit the highest co-occurrence rates, suggesting frequent co-occurrence between 1-day extremes and peak 3-day totals. In contrast, regions such as the Ohio Valley (57%) and the Southeast (59%) show slightly lower co-occurrence, indicating somewhat weaker alignment between single-day maxima and peak 3-day totals. For the 5-day duration (green), co-occurrence frequencies remain high but are consistently lower than for the 3-day duration, with mean frequencies ranging from 55 to 63%. This suggests a modest decrease in co-occurrence between 1-day and multi-day extremes as the accumulation window increases. This trend is consistent with [Supplementary Table S4](#), where mean co-occurrence values decrease from 3-day to 5-day durations in every climate region. Co-occurrence is lowest when comparing MAX1D to the maximum MAXWD (CM1MWD in blue), with mean frequencies ranging from 9 to 25%. This indicates that, in most years, the MAX1D does not coincide with the overall wettest-day sequence. The West (mean = 25%) and Southwest (17%) exhibit the highest co-occurrence in this category, while the Northeast (9%) and Upper Midwest (10%) are the lowest. Wet-spell accumulations reflect stochastic and variable-duration events; thus, the consistently low alignment across regions highlights a structural distinction between single-day maxima and event-based accumulation extremes.

Taken together, these results indicate that while 55–65% of MAX1D events are embedded within MAX3D or MAX5D durations, a substantial portion of multi-day extremes (35–45%) occurs independently of the annual MAX1D. The divergence is most pronounced for MAXWD, where 75–90% of wet-spell accumulations do not coincide with the MAX1D event. These findings highlight that MAX1D extremes alone may not fully represent the structure of multi-day precipitation processes across regions.

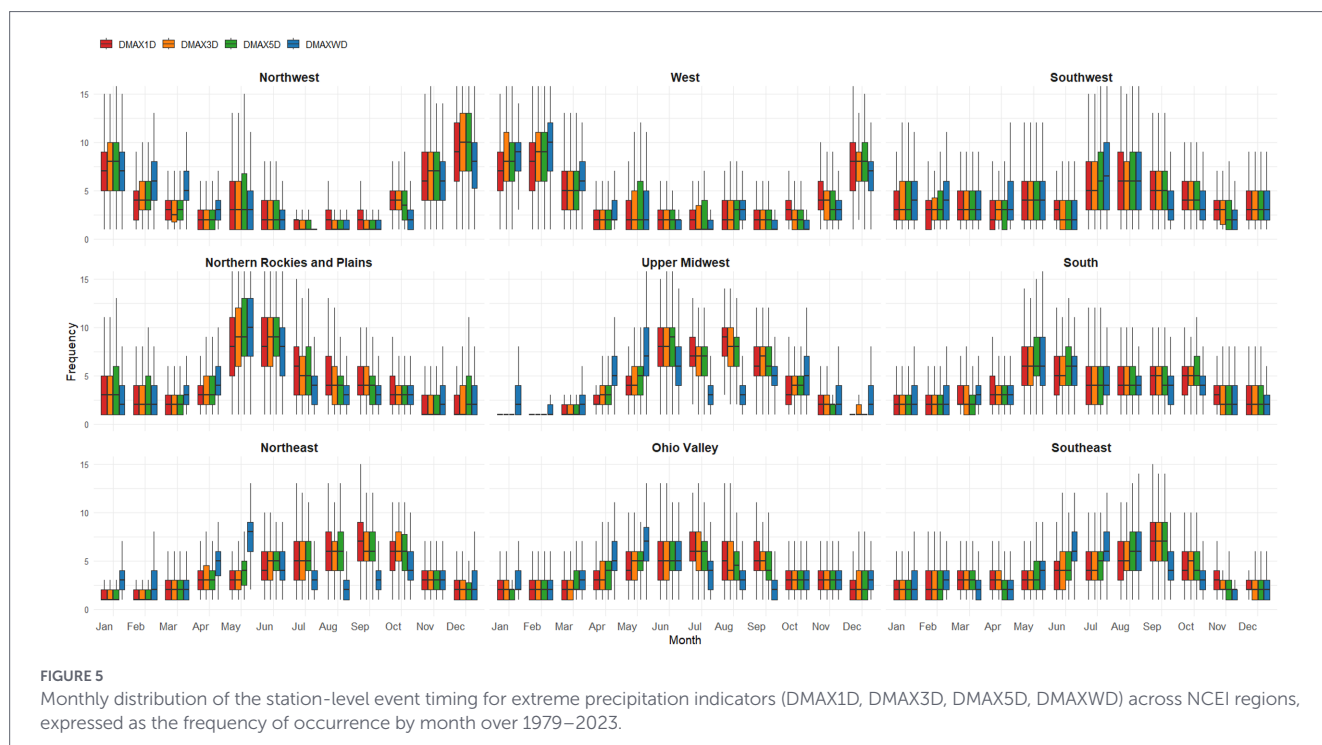
3.2 Seasonality and temporal patterns

3.2.1 Seasonal timing of extremes

[Figure 5](#) presents the monthly distribution of extreme precipitation event frequencies across the nine NCEI climate regions, disaggregated by four event-duration indicators: DMAX1D, DMAX3D, DMAX5D, and DMAXWD (as defined in [Table 1](#)). Each boxplot shows the spread of station-level frequencies, providing a detailed view of how event occurrence varies across both time and space.

A distinct seasonal pattern emerges across regions, showing both similarities and unique regional signatures. The Northwest and West display distinctly different temporal behavior compared to the rest of the country, with peak frequencies during the cool season—notably November to March. Within this pattern, West peaks from December through March, while the Southwest peaks mainly from November and January, with smaller increases in May across most indicators. In addition, DMAXWD shows small jumps between February–March in the Northwest and West, suggesting the influence of extended wet spells. In contrast, most other regions exhibit warm-season dominance. The Upper Midwest and Northern Rockies and Plains show sharp peaks between May and June/July, whereas the Ohio Valley and South display a longer active season from May through September or October. Notably, the Northern Rockies and Plains record the highest peak monthly frequencies among all regions, while the Northwest leads during the cool season.

The seasonal distinction becomes more complex when comparing event-duration indicators. While DMAX1D, DMAX3D, and DMAX5D relatively follow similar temporal patterns in each region, DMAXWD behaves differently in several regions. For example, in the Northeast, DMAXWD peaks in May, whereas DMAX3D and DMAX5D peak later in August and September. Similarly, in the Upper Midwest and Northwest, DMAXWD shows sudden frequency



increases between adjacent months, especially from May to June, compared to the smoother transitions observed in the other indicators.

Taken together, the monthly frequency distribution reveals clear regional contrasts and differences among the duration-based indicators. Identifying these peak months and distinguishing between abrupt versus gradual transitions provides insights into the timing and nature of hydrologic extremes across the U.S.—supporting targeted regional assessments, seasonal forecasting, and adaptation planning.

The seasonal distribution ([Supplementary Figure S1](#)) reinforces the patterns. In most regions, particularly the Northern Rockies and Plains, the Upper Midwest, the Ohio Valley, the South, and the Southeast, the highest frequencies occur during JJA. Conversely, the Northwest and West are dominated by DJF frequencies across all indicators. Seasonal contrast across indicators is also evident: while DMAX1D through DMAX5D tend to peak in JJA, DMAXWD displays a more varied seasonal pattern, with higher frequencies during DJF in the Northwest, West, and parts of the Upper Midwest. These seasonal summaries validate the region and indicator specific timing observed in the monthly plot.

In summary, extreme precipitation timing varies markedly across regions and seasons. Warm-season peaks dominate much of the central and eastern U.S., while cool-season events prevail in the West and Northwest. In several regions, wet-spell events peak at different times than block-duration extremes, emphasizing that precipitation extremes are shaped by distinct meteorological regimes across regions and times of year.

3.2.2 Temporal variability and exploratory trends

To examine potential temporal changes in precipitation extremes, we evaluated seasonal distributions of Kendall's τ values derived from Mann–Kendall trend tests for MAX1D, MAX3D, MAX5D, and MAXWD (detailed results and figures are provided in the [Supplementary Figures S2–S9](#)). Across regions and traditional seasons

(DJF, MAM, JJA, and SON), fewer than approximately 20% of stations exhibit statistically significant monotonic trends. Given this limited statistical robustness, interpretation emphasizes directional tendencies in τ distributions rather than evidence of regionally coherent change. Non-significant results indicate no statistical evidence of monotonic change at those stations.

Across seasons, τ distributions exhibit substantial spatial heterogeneity, with many regions displaying bimodal or broadly dispersed patterns. In DJF and MAM, several northern and eastern regions show distributions skewed toward positive τ values, while parts of the western U.S. display distributions skewed toward negative τ values. During JJA and SON, regional contrasts in τ distributions become more pronounced in some areas, though directional tendencies remain heterogeneous and largely non-significant at the station level.

Across indicators, multi-day extremes (MAX3D, MAX5D, and MAXWD) do not exhibit a consistent duration-dependent pattern in τ distributions relative to MAX1D. In some regions and seasons, directional tendencies are similar across indicators, whereas in others they diverge. No indicator shows spatially uniform or systematically stronger monotonic trends across regions. The dispersion and frequent bimodality of τ values suggest considerable local heterogeneity.

Overall, these results are interpreted as exploratory diagnostics of seasonal and regional patterning in trend direction and should not be construed as formal detection, attribution, or evidence of regionally consistent climate-driven change.

4 Discussion

This study provides a nationwide assessment of extreme precipitation variability across nine U.S. NCEI climate regions, using multiple indicators that span single-day and multi-day extremes. By integrating regional, temporal, and structural perspectives, the results reveal

pronounced heterogeneities in precipitation variability and event characteristics. Beyond documenting regional patterns, this study provides a unified, observation-based diagnostic comparison of variability, intra-event concentration, and co-occurrence across multiple accumulation durations, applied consistently across all nine NCEI climate regions. In this section, we discuss and interpret the main results, which encompass regional variability, event structure, and seasonal and temporal dynamics, and then consider their broader implications for hydrologic design and climate adaptation.

4.1 Regional variability in extreme precipitation

Across most climate regions, shorter-duration extremes (MAX1D, MAX3D) exhibit greater variability than longer-duration accumulations (MAX5D). This pattern is strongest in the Northeast, Southeast, and Upper Midwest, where effect sizes exceeded 0.5, indicating substantially higher variability in shorter events. However, variability is more uniform in the South, Southwest, and West, where effect sizes approach zero or are negative. Across all regions, MAXWD generally shows higher variability than block-duration indicators, with the magnitude of this contrast varying regionally. This behavior is physically consistent with the inherently stochastic, variable-duration nature of wet-spell events, which contributes to greater variability in persistence-based precipitation accumulation compared with fixed-window totals.

The regional contrasts are consistent with previously documented differences in dominant storm types and precipitation-generating processes reported in prior studies. Shorter-duration extremes (MAX1D, MAX3D) are typically generated by convective storms and localized mesoscale systems, resulting in high variability at daily scales (Schumacher and Johnson, 2009; Morales et al., 2015; Nielsen and Schumacher, 2020). In contrast, multi-day extremes such as MAX5D and MAXWD are commonly associated with persistent, synoptic-scale circulation features, including extratropical cyclones, atmospheric rivers, and tropical systems, whose dominance varies regionally (Luong et al., 2017; Bentley et al., 2019; Sinclair et al., 2020; McErlich et al., 2023; Büeler et al., 2024; Haberlie et al., 2024). For instance, previous studies have shown that frontal systems often drive extremes in the Midwest and Northeast (Kunkel et al., 2012; Pfahl and Wernli, 2012), atmospheric rivers frequently underpin long-duration extremes in the West and Northwest (Ralph et al., 2019; Moore et al., 2021), and tropical cyclones can contribute substantially to multi-day extremes in the Gulf and Southeast (Knight and Davis, 2009; Tan et al., 2023). In the Southwest, monsoonal convection and tropical moisture have been identified as significant contributors to extreme precipitation (Favors and Abatzoglou, 2013; Duan et al., 2024). Taken together, the results indicate that relationships between extreme precipitation magnitude and accumulation length vary regionally, and that uniform scaling assumptions may not represent extremes consistently across all regions. Explicit modeling of exogenous drivers using covariate-based or stochastic frameworks (e.g., Koutsoyiannis, 2025) represents a complementary avenue for future research.

Approaches that assume uniform rainfall scaling—such as conventional intensity–duration–frequency (IDF) relationships—may not fully represent regional contrasts in duration-dependent variability, particularly in areas dominated by short-duration convective storms or regions where persistent wet spells drive extreme events. To better

represent local hydrometeorological realities, future flood-risk frameworks may benefit from integrating region-specific storm climatology and explicitly considering the differing behaviors of extremes (Villarini and Smith, 2010; Smith et al., 2011; Ragno et al., 2018; Coelho et al., 2022; Breverman, 2024; Nguyen et al., 2025). In parallel, mixed-population and multi-mechanism statistical approaches offer a promising pathway to represent extremes generated by different physical processes. Such approaches have been applied in hydrological frequency analysis to address mixed storm populations and have been shown to improve, in several cases, the characterization of flood behavior (Ragno et al., 2018; Villarini and Smith, 2010; Smith et al., 2011; Breverman, 2024).

4.2 Event structure and contributions

Across most climate regions, the wettest day within each event contributes disproportionately to multi-day totals, accounting for approximately 70% of the total for CWM3D and 60% for CWM5D. However, this dominance declines with increasing duration, with CWMWD values typically ranging between 25 and 48%. Wettest day dominance is strongest in the Northeast, South, and Upper Midwest, which also show wide variability among stations, while the Northwest and West exhibit more even multi-day distributions. According to Figure 3, right-skewed CWM3D densities cluster above 50%, whereas CWM5D and CWMWD shift leftward, especially in the Northwest, indicating persistent multi-day rainfall. Secondary peaks, where a single 1-day contributes nearly the entire total within a multi-day event, are most noticeable in shorter-duration events (CWM3D) and are often associated with landfalling tropical cyclones or slow-moving mesoscale convective systems (Schumacher and Johnson, 2009; Kunkel et al., 2010; Prat and Nelson, 2016).

Co-occurrence analysis (Figure 4) shows that the annual MAX1D aligns with the wettest day of MAX3D in roughly 60% of station-years, but co-occurrence declines for longer durations and is minimal for MAXWD (only 9–25%). Based on the analyses of wettest single-day contributions and co-occurrence frequencies (Figures 3, 4), many multi-day extremes arise from the accumulation of multiple days rather than a single burst, especially for MAXWD, where the wettest day typically contributes less than 50%. Regions dominated by convective storms (e.g., South, Southeast, Ohio Valley) tend to exhibit sharp peaks, where a single day drives both the 1-day and multi-day extremes. By contrast, regions shaped by frontal systems or atmospheric rivers (e.g., Northwest, West, Northeast) produce steadier, multi-day rainfall distributions (Ralph et al., 2019; Moore et al., 2021). From a hydrologic standpoint, concentrated single-day events heighten flash-flood risk, whereas multi-day accumulations drive soil saturation, landslides, and reservoir inflows (Dougherty and Rasmussen, 2019). The weak correspondence between MAX1D and MAXWD underscores that daily maxima alone are insufficient to represent the structure of flood-generating precipitation across regions. Consistent with Figure 2 and Supplementary Table S3, about 40–70% of the total 3-day and 5-day rainfall typically originates from non-peak days, indicating that daily maxima alone do not adequately represent flood-generating precipitation. Previous studies suggest that shifts in storm persistence and clustering under a warming climate could further alter the balance between single-day and distributed rainfall (Du et al., 2022; Liu et al., 2025).

The event structure patterns observed above are further modulated by seasonal timing and long-term variability, which characterize

the seasonal distribution and temporal organization of these extremes throughout the year.

4.3 Seasonality and temporal dynamics

Seasonal patterns suggest a clear east–west contrast and seasonal asymmetry across the U.S. In the central and eastern regions, extremes peak during summer (JJA), reflecting dominance of convective storms and mesoscale convective systems (Schumacher and Johnson, 2009; Morales et al., 2015; Nielsen and Schumacher, 2018; Nielsen and Schumacher, 2020), while in the Northwest and West, cool-season (DJF) extremes are tied to landfalling atmospheric rivers (Moore et al., 2021; Ralph et al., 2019). The Northern Rockies and Plains show the highest seasonal peak frequencies in the warm season, with a rapid onset in June across all duration indicators, consistent with a transition from snowmelt-driven processes to convective rainfall (Dougherty and Rasmussen, 2019; Feng et al., 2019). In comparison, the Northeast and Ohio Valley demonstrate a more gradual increase beginning in April–May, reflecting the mixed influence of synoptic-scale systems and emerging convection (Kunkel et al., 2012; Dougherty and Rasmussen, 2019).

Wet-spell indicators exhibit some distinct seasonal behavior compared to block-duration extremes. In several regions, their peaks occur in months that do not coincide with the peak of other indicators or show less consistent timing. For instance, MAXWD peaks earlier in the Northeast and increases abruptly from May to June in the Northwest and Upper Midwest, while other extreme indicators follow smoother and more predictable transitions. These offsets and irregularities suggest that wet-spell extremes capture variability in rainfall persistence across consecutive wet days, although individual events may range from strongly clustered multi-day accumulations to shorter-duration episodes within a wet period, which may not align as closely with the seasonal timing of peak daily-intensity indicators. Consequently, wet-spell indicators characterize a different aspect of hydroclimatic variability—one related to event duration and temporal sequencing rather than instantaneous daily intensity.

Seasonal distributions of Kendall's τ values (Supplementary Figures S2–S9) show heterogeneous directional tendencies across regions, seasons, and accumulation durations. However, as fewer than ~20% of stations exhibit statistically significant monotonic trends, these patterns are interpreted as exploratory distributional tendencies rather than spatially coherent or robust regional changes, and they are not used to infer intensification or weakening, or attribute drivers.

For hydrology, these results emphasize that both timing and persistence influence flood risk. Alignment of extreme precipitation with antecedent conditions—such as snowpack, frozen ground, or saturated soils—can amplify runoff generation (Wasko et al., 2020; Berghuijs and Slater, 2023). From a climate perspective, regional and seasonal differences in the τ distributions suggest that thermodynamic and circulation influences may manifest differently across the U.S., although formal detection and attribution are beyond the scope of this study.

5 Conclusion

This study provides a nationwide diagnostic assessment of extreme precipitation variability across nine U.S. NCEI climate regions using complementary indicators that span single-day, fixed multi-day,

and event-based wet-spell extremes. Results show clear regional and duration-dependent contrasts in precipitation behavior: short-duration extremes tend to exhibit greater spatial variability in convectively dominated regions, whereas multi-day and wet-spell extremes highlight the importance of precipitation persistence across much of the U.S.

Across regions, precipitation variability and trend distributions show distinct spatial and seasonal contrasts. However, because statistically significant monotonic trends occur at fewer than ~20% of stations, these patterns are interpreted as exploratory distributional tendencies rather than evidence of widespread change or attribution. The bimodal and skewed structure of trend distributions highlights strong local heterogeneity in recent precipitation behavior.

These findings emphasize that flood-risk assessments must account not only for event intensity but also for rainfall timing, duration, and persistence. By integrating single-day and multi-day indicators, this study provides a regionally nuanced understanding of flood-generating processes and highlights key pathways toward climate-resilient design and adaptation, including the need for multi-day duration frameworks, cross-scale process integration, and explicit coupling between meteorological and hydrologic systems.

5.1 Key findings

- Duration matters: variability does not decrease uniformly from 1-day to 5-day extremes; the magnitude and direction of duration-dependent variability differ across NCEI regions.
- Wet-spell extremes exhibit higher variability: event-based MAXWD exhibits greater variability than fixed-window maxima, reflecting stochastic wet-spell duration and highlighting persistence as a distinct dimension of extremes.
- Multi-day structure is not dominated solely by daily maxima: 40–70% of 3–5 day totals typically arise from non-peak days, and MAX1D aligns weakly with MAXWD in most regions.
- Seasonal timing is region- and duration-dependent: cool-season peaks dominate the West, whereas warm-season peaks characterize much of the central and eastern U.S., with additional differences among accumulation durations.
- Trends are heterogeneous and mostly non-significant: fewer than ~20% of stations show statistically significant monotonic trends, indicating limited evidence for widespread monotonic change in this sample.

The main advance is a consistent, regionally resolved comparison of (i) variability across fixed windows and event-based wet spells, and (ii) intra-event concentration and co-occurrence, using a unified observational framework across all nine NCEI regions. This identifies where daily maxima are representative of multi-day extremes and where persistence-driven accumulation dominates—information directly relevant to multi-duration design and flood-risk characterization.

This study characterizes extreme precipitation using annual and seasonal maxima across multiple accumulation durations, an approach well suited to event-based hydrologic risk assessment, flood hazard analysis, and design-relevant applications. While maxima effectively capture the structure and timing of the most impactful events, they may be sensitive to rare outliers at individual stations. Complementary formulations based on high-percentile thresholds (e.g., 95th or 99th percentile daily or multi-day precipitation), which are widely used in climate monitoring, trend

detection, and impact screening, provide an alternative perspective by characterizing changes across the broader upper tail of the distribution. While percentile-based metrics may moderate the influence of single outlier events, the extent to which they would alter the spatial and structural contrasts identified here remains an open question and warrants dedicated evaluation. Evaluating how maxima-based and percentile-based indicators jointly describe the spatial, temporal, and structural characteristics of multi-duration precipitation extremes represents an important direction for future research.

To advance a process-based understanding of how precipitation persistence and storm mechanisms produce flood-generating extremes, future research should couple these precipitation indicators with climate-variability modes (e.g., ENSO, NAO, PDO), projected storm-track changes, and relevant moisture- and temperature-based indices. In addition, formal event-type classification and covariate-based modeling frameworks could help clarify the physical drivers of persistence and clustering.

Data availability statement

The original contributions presented in the study are included in the article/[Supplementary material](#), further inquiries can be directed to the corresponding author.

Author contributions

SE: Formal analysis, Writing – review & editing, Writing – original draft, Data curation, Software, Resources, Conceptualization, Methodology, Investigation, Visualization, Validation. DS: Supervision, Project administration, Writing – review & editing. AD: Validation, Writing – review & editing.

Funding

The author(s) declared that financial support was not received for this work and/or its publication.

References

- Addisu, S., Selassie, Y. G., Fissaha, G., and Gedif, B. (2015). Time series trend analysis of temperature and rainfall in Lake Tana sub-basin, Ethiopia. *Environ. Syst. Res.* 4:25. doi: 10.1186/s40068-015-0051-0
- Agbonaye, A. I., and Izinyon, O. C. (2021). Evaluating the quality of spatial data for the analysis of climate variability in the coastal region of Nigeria. *Niger. J. Environ. Sci. Technol.* 5, 76–90. doi: 10.36263/nijest.2021.01.0236
- Association of State Dam Safety Officials. (2013). Front range flood (Colorado, 2013). Available online at: <https://damfailures.org/case-study/front-range-flood-colorado-2013> (Accessed October 15, 2025).
- Banerjee, A., Kemter, M., Goswami, B., Merz, B., Kurths, J., and Marwan, N. (2023). Spatial coherence patterns of extreme winter precipitation in the United States. *Theor. Appl. Climatol.* 152, 385–395. doi: 10.1007/s00704-023-04393-5
- Bentley, A. M., Bosart, L. F., and Keyser, D. (2019). A climatology of extratropical cyclones leading to extreme weather events over central and eastern North America. *Mon. Weather Rev.* 147, 1471–1490. doi: 10.1175/MWR-D-18-0453.1
- Berghuijs, W. R., and Slater, L. J. (2023). Groundwater shapes North American river floods. *Environ. Res. Lett.* 18:034043. doi: 10.1088/1748-9326/acbecc
- Bevacqua, E., De Michele, C., Manning, C., Couasnon, A., Ribeiro, A. F., Ramos, A. M., et al. (2021). Guidelines for studying diverse types of compound weather and climate events. *Earth's Future* 9:e2021EF002340. doi: 10.1029/2021EF002340
- Brandi, A., Balling, R. C., Iniguez, P., and Georgescu, M. (2023). Climatological trends of mean and extreme daily precipitation in Arizona (USA). *J. Arid Environ.* 219:105083. doi: 10.1016/j.jaridenv.2023.105083
- Breverman, A. (2024). Addressing mixed populations in flood frequency analyses: a case study in Eastern Pennsylvania. U.S. Army Corps of Engineers, SEDHYD Conference Paper. Available online at: https://www.hec.usace.army.mil/confluence/sspdocs/ssptr/files/105580369/213684392/1/1728072320244/SEDHYD_Breverman_Bartles_Karlovits_Mixed_Populations_Lehigh_River.pdf (Accessed October 15, 2025).
- Brunner, M. I., Slater, L. J., Tallaksen, L. M., and Clark, M. (2021). Challenges in modeling and predicting floods and droughts: a review. *Wiley Interdiscip. Rev. Water* 8:e1520. doi: 10.1002/wat2.1520

Acknowledgments

The research was conducted by Dewberry with the goal of advancing the state of science in hydrometeorology.

Conflict of interest

SE, DS, and AD were employed by Integrated Resilience Solutions, Dewberry.

Generative AI statement

The author(s) declared that Generative AI was not used in the creation of this manuscript.

Any alternative text (alt text) provided alongside figures in this article has been generated by Frontiers with the support of artificial intelligence and reasonable efforts have been made to ensure accuracy, including review by the authors wherever possible. If you identify any issues, please contact us.

Publisher's note

All claims expressed in this article are solely those of the authors and do not necessarily represent those of their affiliated organizations, or those of the publisher, the editors and the reviewers. Any product that may be evaluated in this article, or claim that may be made by its manufacturer, is not guaranteed or endorsed by the publisher.

Supplementary material

The Supplementary material for this article can be found online at: <https://www.frontiersin.org/articles/10.3389/frwa.2026.1753501/full#supplementary-material>

- Büeler, D., Sprenger, M., and Wernli, H. (2024). Northern hemisphere extratropical cyclone biases in ECMWF subseasonal forecasts. *Q. J. R. Meteorol. Soc.* 150, 1096–1123. doi: 10.1002/qj.4638
- Changnon, S. A., Kunkel, K. E., and Andsager, K. (2001). Causes for record high flood losses in the Central United States. *Water Int.* 26, 223–230. doi: 10.1080/02508060108686908
- Clark, M. P., Schaeffli, B., Schymanski, S. J., Samaniego, L., Luce, C. H., Jackson, B. M., et al. (2016). Improving the theoretical underpinnings of process-based hydrologic models. *Water Resour. Res.* 52, 2350–2365. doi: 10.1002/2015WR017910
- Coelho, G. D. A., Ferreira, C. M., Johnston, J., Kinter, J. L. III, Dollan, I. J., and Maggioni, V. (2022). Potential impacts of future extreme precipitation changes on flood engineering design across the contiguous United States. *Water Resour. Res.* 58:e2021WR031432. doi: 10.1029/2021WR031432
- Dettinger, R. D., and Horton, D. E. (2023). Observed changes in interannual precipitation variability in the United States. *Geophys. Res. Lett.* 50:e2023GL104533. doi: 10.1029/2023GL104533
- Dharmarathne, G., Waduge, A. O., Bogahawaththa, M., Rathnayake, U., and Meddage, D. P. P. (2024). Adapting cities to the surge: a comprehensive review of climate-induced urban flooding. *Results Eng.* 22:102123. doi: 10.1016/j.rineng.2024.102123
- Dhawale, R., Schuster-Wallace, C. J., and Pietroniro, A. (2024). Assessing the multidimensional nature of flood and drought vulnerability index: a systematic review of literature. *Int. J. Disaster Risk Reduct.* 112:104764. doi: 10.1016/j.ijdrr.2024.104764
- Dougherty, E., and Rasmussen, K. L. (2019). Climatology of flood-producing storms and their associated rainfall characteristics in the United States. *Mon. Weather Rev.* 147, 3861–3877. doi: 10.1175/MWR-D-19-0020.1
- Du, H., Donat, M. G., Zong, S., Alexander, L. V., Manzanar, R., Kruger, A., et al. (2022). Extreme precipitation on consecutive days occurs more often in a warming climate. *Bull. Am. Meteorol. Soc.* 103, E1130–E1145. doi: 10.1175/BAMS-D-21-0140.2
- Duan, S., Ullrich, P., and Boos, W. R. (2024). Meteorological drivers of North American monsoon extreme precipitation events. *J. Geophys. Res. Atmos.* 129:e2023JD040535. doi: 10.1029/2023JD040535
- Durre, I., Menne, M. J., Gleason, B. E., Houston, T. G., and Vose, R. S. (2010). Comprehensive automated quality assurance of daily surface observations. *J. Appl. Meteorol. Climatol.* 49, 1615–1633. doi: 10.1175/2010JAMC2375.1
- Eilander, D., Couasnon, A., Leijnse, T., Ikeuchi, H., Yamazaki, D., Muis, S., et al. (2023). A globally applicable framework for compound flood hazard modeling. *Nat. Hazards Earth Syst. Sci.* 23, 823–846. doi: 10.5194/nhess-23-823-2023
- El Kenawy, A. M. (2024). “Hydroclimatic extremes in arid and semi-arid regions: status, challenges, and future outlook,” in *Hydroclimatic Extremes in the Middle East and North Africa*, Eds. E. S. M. Robaa and M. M. M. Torab, (Amsterdam, Netherlands: Elsevier), 1–22.
- Favors, J. E., and Abatzoglou, J. T. (2013). Regional surges of monsoonal moisture into the southwestern United States. *Mon. Weather Rev.* 141, 182–191. doi: 10.1175/MWR-D-12-00037.1
- Feng, Z., Houze, R. A. Jr., Leung, L. R., Song, F., Hardin, J. C., Wang, J., et al. (2019). Spatiotemporal characteristics and large-scale environments of mesoscale convective systems east of the Rocky Mountains. *J. Clim.* 32, 7303–7328. doi: 10.1175/JCLI-D-19-0137.1
- Fereshtehpour, M., Najafi, M. R., and Cannon, A. J. (2025). Characterizing compound inland flooding mechanisms and risks in North America under climate change. *Earth's Future* 13:e2024EF005353. doi: 10.1029/2024EF005353
- Friedrich, K., Kalina, E. A., Aikins, J., Steiner, M., Gochis, D., Kucera, P. A., et al. (2016). Raindrop size distribution and rain characteristics during the 2013 great Colorado flood. *J. Hydrometeorol.* 17, 53–72. doi: 10.1175/JHM-D-14-0184.1
- Ganguli, P., Lin, N., and Wendi, D. (2022). Multivariate extremes and compound, interconnected, and cascading events: understanding the past and projections into the future. *Front. Water* 4:1052694. doi: 10.3389/frwa.2022.1052694
- Gochis, D., Schumacher, R., Friedrich, K., Doesken, N., Kelsch, M., Sun, J., et al. (2015). The great Colorado flood of September 2013. *Bull. Am. Meteorol. Soc.* 96, 1461–1487. doi: 10.1175/BAMS-D-13-00241.1
- Haberlie, A. M., Wallace, B., Ashley, W. S., Gensini, V. A., and Michaelis, A. C. (2024). Mesoscale convective system activity in the United States under intermediate and extreme climate change scenarios. *Clim. Chang.* 177:94. doi: 10.1007/s10584-024-03752-z
- Hao, Z. (2022). Compound events and associated impacts in China. *iScience* 25:104689. doi: 10.1016/j.isci.2022.104689
- Heimann, D. C., Holmes, R. R. Jr., and Harris, T. E. (2018). “Flooding in the southern Midwestern United States, April–May 2017,” in *U.S. Geological Survey Open-File Report 2018–1004*, (Reston, VA, USA: U.S. Geological Survey reports).
- Hwang, J., and Lall, U. (2024). Increasing dam failure risk in the USA due to compound rainfall clusters as climate changes. *NPJ Nat. Hazards* 1:27. doi: 10.1038/s44304-024-00027-6
- Jiang, S., Bevacqua, E., and Zscheischler, J. (2022). River flooding mechanisms and their changes in Europe revealed by explainable machine learning. *Hydrol. Earth Syst. Sci.* 26, 6339–6359. doi: 10.5194/hess-26-6339-2022
- Jin, H., Chen, X., Adamowski, J., and Hatami, S. (2024). Determination of duration, threshold, and spatiotemporal distribution of extreme continuous precipitation in nine major river basins in China. *Atmos. Res.* 300:107217. doi: 10.1016/j.atmosres.2023.107217
- Kendall, M. G. (1975). *Rank Correlation Methods*. 4th Edn London, UK: Charles Griffin.
- Knight, D. B., and Davis, R. E. (2009). Contribution of tropical cyclones to extreme rainfall events in the southeastern United States. *J. Geophys. Res. Atmos.* 114, 1–17. doi: 10.1029/2009JD012511
- Koutsoyiannis, D. (2025). *Stochastics of Hydroclimatic Extremes—A Cool Look at Risk*. 5th Edn Athens: Kallipos Open Academic Editions, 420.
- Kraft, L. L., Villarini, G., and Czajkowski, J. (2023). Characterizing the 2019 Midwest flood: a hydrologic and socioeconomic perspective. *Weather Clim. Soc.* 15, 603–617. doi: 10.1175/WCAS-D-22-0065.1
- Kunkel, K. E., Easterling, D. R., Kristovich, D. A., Gleason, B., Stoecker, L., and Smith, R. (2010). Recent increases in U.S. heavy precipitation associated with tropical cyclones. *Geophys. Res. Lett.* 37, 1–4. doi: 10.1029/2010GL045164
- Kunkel, K. E., Easterling, D. R., Kristovich, D. A., Gleason, B., Stoecker, L., and Smith, R. (2012). Meteorological causes of the secular variations in observed extreme precipitation events for the conterminous United States. *J. Hydrometeorol.* 13, 1131–1141. doi: 10.1175/JHM-D-11-0108.1
- Lewis, J. M., and Trevisan, A. R. (2019). “Peak streamflow and stages at selected Streamgages on the Arkansas River in Oklahoma and Arkansas, may to June 2019,” in *U.S. Geological Survey Open-File Report 2019–1129*, (Reston, VA, USA: U.S. Geological Survey reports).
- Liu, Y., Wright, D. B., Quintero, F., Michalek, A., Villarini, G., and Smith, J. A. (2025). Increasing flood hazard in the lower Mississippi River due to extreme storm clustering. *Sci. Adv.* 11:eadt1868. doi: 10.1126/sciadv.adt1868
- Luong, T. M., Castro, C. L., Chang, H. I., Lahmers, T., Adams, D. K., and Ochoa-Moya, C. A. (2017). The more extreme nature of north American monsoon precipitation in the southwestern United States as revealed by a historical climatology of simulated severe weather events. *J. Appl. Meteorol. Climatol.* 56, 2509–2529. doi: 10.1175/JAMC-D-16-0358.1
- Luong, T. T., Pöschmann, J., Kronenberg, R., and Bernhofer, C. (2021). Rainfall threshold for flash flood warning based on model output of soil moisture: case study Wernersbach, Germany. *Water* 13:1061. doi: 10.3390/w13081061
- Ma, K., Feng, D., Lawson, K., Tsai, W. P., Liang, C., Huang, X., et al. (2021). Transferring hydrologic data across continents—leveraging data-rich regions to improve hydrologic prediction in data-sparse regions. *Water Resour. Res.* 57:e2020WR028600. doi: 10.1029/2020WR028600
- Mann, H. B. (1945). Non-parametric tests against trend. *Econometrica* 13, 245–259. doi: 10.2307/1907187
- McErlach, C., McDonald, A., Renwick, J., and Schuddeboom, A. (2023). An assessment of extra-tropical cyclone precipitation extremes over the southern hemisphere using ERA5. *Geophys. Res. Lett.* 50:e2023GL104130. doi: 10.1029/2023GL104130
- Menne, M. J., Durre, I., Vose, R. S., Gleason, B. E., and Houston, T. G. (2012). An overview of the global historical climatology network—daily database. *J. Atmos. Ocean. Technol.* 29, 897–910. doi: 10.1175/JTECH-D-11-00103.1
- Moges, E., Ruddell, B. L., Zhang, L., Driscoll, J. M., and Larsen, L. G. (2022). Strength and memory of precipitation’s control over streamflow across the conterminous United States. *Water Resour. Res.* 58:e2021WR030186. doi: 10.1029/2021WR030186
- Moore, B. J., White, A. B., and Gottas, D. J. (2021). Characteristics of long-duration heavy precipitation events along the west coast of the United States. *Mon. Weather Rev.* 149, 2255–2277. doi: 10.1175/MWR-D-20-0336.1
- Morales, A., Schumacher, R. S., and Kreidenweis, S. M. (2015). Mesoscale vortex development during extreme precipitation: Colorado, September 2013. *Mon. Weather Rev.* 143, 4943–4962. doi: 10.1175/MWR-D-15-0086.1
- National Oceanic and Atmospheric Administration. (2019). Overview of events—Midwest Region heavy precipitation and flooding of 2019. Available online at: https://www.ncei.noaa.gov/sites/default/files/MW-2019_Final.pdf (Accessed October 15, 2025).
- National Oceanic and Atmospheric Administration, National Weather Service. (2025). Flood related hazards. Available online at: <https://www.weather.gov/safety/flood-hazards> (Accessed October 14, 2025).
- Neal, R. A., and Phillips, I. D. (2011). Winter daily precipitation variability over Cumbria, Northwest England. *Theor. Appl. Climatol.* 106, 245–262. doi: 10.1007/s00704-011-0483-z
- Nguyen, T., Kravitz, B., O’Brien, T. A., Ficklin, D. L., Rasmussen, K. L., Kruczkiwicz, A., et al. (2025). Future intensity–duration–frequency curves of extreme precipitation in the Midwest United States from convection-permitting modeling. *J. Geophys. Res. Atmos.* 130:e2024JD042798. doi: 10.1029/2024JD042798
- Nielsen, E. R., and Schumacher, R. S. (2018). Dynamical insights into extreme short-term precipitation associated with supercells and mesovortices. *J. Atmos. Sci.* 75, 2983–3009. doi: 10.1175/JAS-D-17-0385.1
- Nielsen, E. R., and Schumacher, R. S. (2020). Observations of extreme short-term precipitation associated with supercells and mesovortices. *Mon. Weather Rev.* 148, 159–182. doi: 10.1175/MWR-D-19-0146.1
- NOAA Weather Forecast Office. (2025). River flooding. Available online at: <https://www.weather.gov/source/lzk/annual/2019event4.htm> (Accessed October 15, 2025).

- Pfahl, S., and Wernli, H. (2012). Quantifying the relevance of cyclones for precipitation extremes. *J. Clim.* 25, 6770–6780. doi: 10.1175/JCLI-D-11-00705.1
- Pournasiri, M. P., and Pal, I. (2016). Patterns of hydrological drought indicators in major U.S. river basins. *Clim. Chang.* 134, 549–563. doi: 10.1007/s10584-015-1542-8
- Pournasiri, M. P., Towler, E., and Pal, I. (2018). Characterizing and understanding the variability of streamflow drought indicators within the USA. *Hydrol. Sci. J.* 63, 1791–1803. doi: 10.1080/02626667.2018.1534240
- Prat, O. P., and Nelson, B. R. (2016). On the link between tropical cyclones and daily rainfall extremes derived from global satellite observations. *J. Clim.* 29, 6127–6135. doi: 10.1175/JCLI-D-16-0289.1
- Ragno, E., AghaKouchak, A., Love, C. A., Cheng, L., Vahedifard, F., and Lima, C. H. (2018). Quantifying changes in future intensity–duration–frequency curves using multi-model ensemble simulations. *Water Resour. Res.* 54, 1751–1764. doi: 10.1002/2017WR021975
- Ralph, F. M., Rutz, J. J., Cordeira, J. M., Dettinger, M., Anderson, M., Reynolds, D., et al. (2019). A scale to characterize the strength and impacts of atmospheric rivers. *Bull. Am. Meteorol. Soc.* 100, 269–289. doi: 10.1175/BAMS-D-18-0023.1
- Roque-Malo, S., and Kumar, P. (2017). Patterns of change in high-frequency precipitation variability over North America. *Sci. Rep.* 7:10853. doi: 10.1038/s41598-017-10827-8
- Schumacher, R. S., and Johnson, R. H. (2009). Quasi-stationary, extreme-rain-producing convective systems associated with midlevel cyclonic circulations. *Weather Forecast.* 24, 555–574. doi: 10.1175/2008WAF222173.1
- Serinaldi, F., Kilsby, C. G., and Lombardo, F. (2018). Untenable nonstationarity: an assessment of the fitness for purpose of trend tests in hydrology. *Adv. Water Resour.* 111, 132–155. doi: 10.1016/j.advwatres.2017.10.015
- Shapiro, S. S., and Wilk, M. B. (1965). An analysis of variance test for normality (complete samples). *Biometrika* 52, 591–611. doi: 10.1093/biomet/52.3-4.591
- Shen, M., and Chui, T. F. M. (2023). Quantifying the relative contributions of different flood-generating mechanisms to floods across CONUS. *J. Hydrol.* 626:130255. doi: 10.1016/j.jhydrol.2023.130255
- Sinclair, V. A., Rantanen, M., Haapanala, P., Räisänen, J., and Järvinen, H. (2020). The characteristics and structure of extra-tropical cyclones in a warmer climate. *Weather Clim. Dynam.* 1, 1–25. doi: 10.5194/wcd-1-1-2020
- Smith, J. A., Villarini, G., and Baeck, M. L. (2011). Mixture distributions and the hydroclimatology of extreme rainfall and flooding in the eastern United States. *J. Hydrometeorol.* 12, 294–309. doi: 10.1175/2010JHM1242.1
- Stein, L., Pianosi, F., and Woods, R. (2020). Event-based classification for global study of river flood-generating processes. *Hydrol. Process.* 34, 1514–1529. doi: 10.1002/hyp.13678
- Tan, M. L., Armanuos, A. M., Ahmadianfar, I., Demir, V., Heddum, S., Al-Areeq, A. M., et al. (2023). Evaluation of NASA POWER and ERA5-land for estimating tropical precipitation and temperature extremes. *J. Hydrol.* 624:129940. doi: 10.1016/j.jhydrol.2023.129940
- Tarasova, L., Lun, D., Merz, R., Blöschl, G., Basso, S., Bertola, M., et al. (2023). Shifts in flood generation processes exacerbate regional flood anomalies in Europe. *Commun. Earth Environ.* 4:49. doi: 10.1038/s43247-023-00714-8
- Tramblay, Y., Villarini, G., Saidi, M. E., Massari, C., and Stein, L. (2022). Classification of flood-generating processes in Africa. *Sci. Rep.* 12:18920. doi: 10.1038/s41598-022-23725-5
- Tye, M. R., and Cooley, D. (2015). A spatial model to examine rainfall extremes in Colorado's front range. *J. Hydrol.* 530, 15–23. doi: 10.1016/j.jhydrol.2015.09.023
- U.S. Environmental Protection Agency. (2025). Extreme precipitation. Available online at: <https://www.epa.gov/climatechange-science/extreme-precipitation> (Accessed October 14, 2025).
- Uccellini, L. W. (2014). The Record Front Range and Eastern Colorado Floods of September 11–17, 2013. NOAA Service Assessment; National Oceanic and Atmospheric Administration: Silver Spring, MD, USA. Available online at: https://www.weather.gov/media/publications/assessments/14colorado_floods.pdf (Accessed October 15, 2025).
- Uchale, N. N., and Singh, B. B. (2025). Characteristics and projected changes in maximum daily precipitation across the globe. *Q. J. R. Meteorol. Soc.* 151:e4912. doi: 10.1002/qj.4912
- Villarini, G., and Smith, J. A. (2010). Flood peak distributions for the eastern United States. *Water Resour. Res.* 46, 1–17. doi: 10.1029/2009WR008395
- Wan, C., Cheng, C., Ye, S., Shen, S., and Zhang, T. (2021). Recognizing the aggregation characteristics of extreme precipitation events using spatio-temporal scanning and the local spatial autocorrelation model. *Atmos.* 12:218. doi: 10.3390/atmos12020218
- Wang, Y. (2025). Spatiotemporal Dynamics and Climate-Driven Risk of Compound Flood Events in the Great Lakes Basin, [Ph.D. Thesis] The University of Western Ontario, London, ON, Canada. Available online at: <https://hdl.handle.net/20.500.14721/38586> (Accessed October 29, 2025).
- Wasko, C., Nathan, R., and Peel, M. C. (2020). Changes in antecedent soil moisture modulate flood seasonality in a changing climate. *Water Resour. Res.* 56:e2019WR026300. doi: 10.1029/2019WR026300
- Western Water Assessment. (2025). Pagosa Springs Rapid Assessment—October 10–14, 2025 Flooding Event. Western Water Assessment: Boulder, CO, USA. Available online at: https://wwa.colorado.edu/sites/default/files/2025-10/Pagosa_Springs_Rapid_Assessment%E2%80%93Final_Publication_102225.pdf (Accessed October 15, 2025).
- Wilcoxon, F. (1945). Individual comparisons by ranking methods. *Biom. Bull.* 1, 80–83. doi: 10.2307/3001968
- Williams, D. J., and Lewis, J. M. (2020). *RiverWare Model Outputs for Flood Calculations along the Arkansas River for a Flood Event in Eastern and Northeastern Oklahoma during May–June 2019*. Austin, TX: USGS. doi: 10.5066/P9T3Q6MB
- Ye, S., Wang, J., Ran, Q., Chen, X., and Liu, L. (2021). The relative importance of antecedent soil moisture and precipitation in flood generation in the middle and lower Yangtze River basin. *Hydrol. Earth Syst. Sci.* 26, 4919–4942. doi: 10.5194/hess-26-4919-2022
- Yeh, H. F., and Chen, H. Y. (2022). Assessing the long-term hydrologic responses of river catchments in Taiwan using a multiple-component hydrograph approach. *J. Hydrol.* 610:127916. doi: 10.1016/j.jhydrol.2022.127916
- Yu, T., Ran, Q., Pan, H., Li, J., Pan, J., and Ye, S. (2023). The impacts of rainfall and soil moisture to flood hazards in a humid mountainous catchment: a modeling investigation. *Front. Earth Sci.* 11:1285766. doi: 10.3389/feart.2023.1285766
- Zhang, W., and Villarini, G. (2020). Deadly compound heat stress–flooding hazard across the Central United States. *Geophys. Res. Lett.* 47:e2020GL089185. doi: 10.1029/2020GL089185
- Zscheischler, J., Sillmann, J., and Alexander, L. (2022). Introduction to the special issue: compound weather and climate events. *Weather Clim. Extrem.* 35:100381. doi: 10.1016/j.wace.2021.100381
- Zscheischler, J., Westra, S., Van Den Hurk, B. J., Seneviratne, S. I., Ward, P. J., Pitman, A., et al. (2018). Future climate risk from compound events. *Nat. Clim. Chang.* 8, 469–477. doi: 10.1038/s41558-018-0156-3

Glossary

CM1M3D - Co-occurrence of MAX1D with the wettest day within the MAX3D

CM1M5D - Co-occurrence of MAX1D with the wettest day within the MAX5D

CM1MWD - Co-occurrence of MAX1D with the wettest day within the MAXWD

CV - Coefficient of variation

CWM3D - Contribution of the wettest day to MAX3D

CWM5D - Contribution of the wettest day to MAX5D

CWMWD - Contribution of the wettest day to MAXWD

DJF - December, January, February

DMAX1D - Date of the annual maximum precipitation

DMAX3D - Date of the wettest day in the maximum 3-day precipitation

DMAX5D - Date of the wettest day in the maximum 5-day precipitation

GHCN-D - Global Historical Climatology Network-Daily

ENSO - El Niño–Southern Oscillation

IDF - Intensity duration frequency

JJA - June, July, August

MAM - March, April, May

MAX1D - Maximum 1-day precipitation

MAX3D - Maximum 3-day precipitation

MAX5D - Maximum 5-day precipitation

MAXWD - MAXWD Maximum precipitation accumulated during the longest wet spell

MK - Mann-Kendall

mm - Millimeter

NAO - North Atlantic Oscillation

NCEI - National Centers for Environmental Information

NOAA - National Oceanic and Atmospheric Administration

PDO - Pacific Decadal Oscillation

PRCP - Precipitation

SD - Standard deviations

SON - September, October, November

U.S. - United States

U.S. EPA - U.S. Environmental Protection Agency

% - Percentage